Cell J
Cell Journal(Yakhteh)
Homepage: https://www.celljournal.org/
Original Article
Vol 25, No 11, November 2023, Pages: 753-763

Osteoblastic Differentiation of Stem Cells from Human Exfoliated Deciduous Teeth by Probiotic Hydroxyapatite

Sabereh Nouri, Ph.D.[1], Rasoul Roghanian, Ph.D.[1]*, Giti Emtiazi, Ph.D.[1], Oguzhan Gunduz, Ph.D.[2], Rasoul Shafiei, Ph.D.[1]

1. Department of Cell, Molecular Biology and Microbiology, Faculty of Biological Science and Technology, University of Isfahan, Isfahan, Iran
2. Center for Nanotechnology and Biomaterials Application and Research at Marmara University, Goztepe Campus, Istanbul, Turkey

Abstract

Objective: Multipotent cells derived from human exfoliated deciduous teeth (SHED) possess the ability to differentiate into various cell types, including osteoblasts. This study aims to simulate the growth induction and osteogenic differentiation of SHED cells using probiotics and their resultant biomaterials.

Materials and Methods: This experimental study proceeded in two stages. Initially, we evaluated the effect of autoclaved nutrient agar (NA) grown probiotic *Bacillus coagulans (B. coagulans)* on the SHED and MG-63 cell lines. Subsequently, probiotics grown on the Pikovskaya plus urea (PVKU) medium and their synthesised hydroxyapatite (HA) were identified using X-ray diffraction (XRD), scanning electron microscopy (SEM), energy-dispersive X-ray (EDX), and Fourier transform infrared spectroscopy (FTIR), and then used to stimulate growth and osteogenic differentiation of the SHED cell line. Osteoblast cell differentiation was assessed by morphological changes, the alkaline phosphatase (ALP) assay, and alizarin red staining.

Results: There was a substantial increase in SHED cell growth of about 14 and 33% due to probiotics grown on NA and PVKU medium, respectively. The PVKU grown probiotics enhanced growth and induced stem cell differentiation due to HA content. Evidence of this differentiation was seen in the morphological shift from spindle to osteocyte-shaped cells after five days of incubation, an increase in ALP level over 21 days, and detection of intracellular calcium deposits through alizarin red staining-all indicative of osteoblast cell development.

Conclusion: The osteogenic differentiation process in stem cells, improved by the nano-HA-containing byproducts of probiotic bacteria in the PVKU medium, represents a promising pathway for leveraging beneficial bacteria and their synthesised biomaterials in tissue engineering.

Keywords: Differentiation, Hydroxyapatite, Osteoblast, Probiotic

Citation: **Nouri S, Roghanian R, Emtiazi G, Gunduz O, Shafiei R. Osteoblastic differentiation of stem cells from human exfoliated deciduous teeth by probiotic hydroxyapatite. Cell J. 2023; 25(11): 753-763. doi: 10.22074/CELLJ.2023.1999743.1276**

Introduction

Each year, bone disorders and defects from skeletal diseases, congenital malformations, trauma, and tumour resections necessitate bone reconstruction. Conventionally, these issues are addressed using metal implants or filling with bio-active materials in medical treatments. It is crucial to have activated calcium phosphate-based materials on the metallic implant's surface or within the filler bone cement in these therapeutic techniques (1, 2). Calcium phosphate salts comprise the primary mineral component of vertebrate bone and teeth, among which hydroxyapatite (HA), the most thermodynamically stable calcium phosphate compound, most closely resembles bone mineral protein, and is composed of up to 70% hard tissue (3, 4). HA has extensive applications in medicine, orthopaedics, dentistry, bone tissue engineering, implant coating, drug delivery systems, and cosmetics, in addition to sanitation, sewage treatment, and the food industry. It is used in dental floss, toothpaste, and food additives to prevent tooth decay and support dental repair (5, 6). Biomaterials that bond with host bone tissues are highly effective in initiating cell regeneration (7). HA can be synthesised through chemical and biological methods, with the current focus of nano-biotechnology on environmentally friendly biosynthesis methods. Among natural HA sources, bacteria can act as bio-manufacturing units for nano-synthesis. This process, known as biomineralisation, yields inorganic crystals while exerting unique control over their morphology and nano-structural texture (8). The best bacterial candidates for biomineralisation are probiotics, the beneficial bacteria that reside in the human body and contribute to its functioning. They have been utilised in sanitation, medicine, and the food industry for several years (9, 10). Because medical usage of nano-HA

Received: 09/April/2023, Revised: 01/August/2023, Accepted: 30/October/2023
***Corresponding Address: P.O.Box: 8174673441 Department of Cell, Molecular Biology and Microbiology, Faculty of Biological Science and Technology, University of Isfahan, Isfahan, Iran**
Email: r.roghanian@sci.ui.ac.ir

Royan Institute
Cell Journal (Yakhteh)

is one of the most important of our requirements, it is critical to derive this nano-particle from a safe bacterial source so that purification and characterisation are not a later issue. When these nanoparticles reach the body, they are likely to cause inflammatory reactions; therefore, the use of pathogenic bacteria to generate nano-HA may enhance the immune response (9).

The gut microbiome plays a crucial role in regulating bone health by influencing both postnatal skeletal development and skeletal involution. Imbalances in microbiota composition and the body's response to these changes contribute to pathological bone loss; adjusting the microbiota composition through interventions like prebiotics and probiotics may help prevent or reverse this loss (11). Numerous studies have demonstrated that dietary changes can enhance bone health and modify the gut microbiota composition. Additionally, recent research has explored strategies that involve bacteria and their components to influence the proliferation and differentiation of mesenchymal stem cells (MSC) (11-13). On the other hand, HA can assist stem cells in differentiating into osteogenic cells, and thus play a significant role in tissue engineering. Equally important to the field of tissue engineering is the type of stem cells employed. Among the most advantageous are stem cells from human exfoliated deciduous teeth (SHED) (14). Deciduous teeth are a set of 20 teeth that emerge after six months of age and are typically replaced between the ages of 6 to 13 years, and they contain viable pulp within their crowns (15). Dental pulp is a jelly-like tissue at the centre of each tooth that contains connective tissue, blood vessels, and odontoblasts. SHED express MSC surface markers such as STRO-1 and CD146. Cells that contain these markers are found around the blood vessels of the pulp, which suggests that SHED may originate from the microenvironment around these vessels (14, 15).

SHED possess the capability to differentiate into odontogenic, osteogenic, neurogenic, adipogenic, myogenic, and chondrogenic lines under suitable conditions. SHED coupled with HA particles and implanted into immunocompromised animals can differentiate into odontoblasts. The capacity for odontogenic differentiation and the ability to stimulate the bone *in vitro* suggest that SHED might constitute a population of multinucleated stem cells (16, 17).

Therefore, deciduous exfoliated teeth could be an excellent source of stem cells to repair damaged tooth structures, stimulate bone regeneration, and perhaps treat neurodegenerative diseases (18). Dental stem cells obtained from extracted teeth receive more attention because isolating these pluripotent cells is relatively simple and does not involve invasive action compared to the usual sources of MSC such as bone marrow or fat (15, 17, 18). One of the most promising sources of tooth stem cells is deciduous teeth, which are lost during puberty. Stem cells from the missing tooth pulp chamber could be isolated and kept as a convenient and painless source for restorative and reconstructive treatments after losing deciduous teeth, and permanent teeth are replaced. SHED stem cells are pluripotent and have rapid proliferative capability. Hence, they are a preferred stem cell source compared to other storable dental stem cells (18).

For HA to qualify as a biomaterial, it must possess biocompatibility and bioactivities such as osteoconductivity and osteoinductivity. Biocompatibility refers to a material's systemic and cellular compatibility with the live body (19).

The separate efficacies of probiotics and HA have been shown in studies conducted on cell cultures that examined the proliferation, mineralisation, and expression of marker genes. These studies revealed that MG-63 cells, when treated with probiotics, exhibited characteristics indicative of their commitment to osteoblasts, including increased proliferation and differentiation (20).

While some studies have examined the influence of bacterial probiotic components on the proliferation and differentiation of stem cells, the primary objective of our present research is to explore the possibility of a safe probiotic [*Bacillus coagulans (B. coagulans*)] to produce non-toxic HA through biomineralisation. Additionally, we aim to assess the potential of probiotic debris, with its synthesised HA as a byproduct, to enhance the multiplication of MG-63 cells and promote proliferation and differentiation in SHED.

Materials and Methods

Production of bacterial synthesised hydroxyapatite

The project was found to be in accordance to the ethical principle and the national norms and standards for conducting Medical Research in Iran (IR.UI.REC.1402.017)

In this experimental study, we cultured a standard probiotic bacterial strain of *B. coagulans* (ATCC 7050) on nutrient agar (NA, Merck, Germany) and Pikovskaya plus urea (PVKU) medium that consisted of 10 g/L dextrose, 5 g/L $Ca_3(PO_4)_2$, 0.2 g/L NaCl, 0.2 g/L KCl, 0.1 g/L $MgSO_4.7H_2O$, 0.5 g/L yeast extract, 0.002 g/L $FeSO_4.7H_2O$, 0.002 g/L $MnSO_4 \cdot H_2O$, 15 g/L agar-agar, (pH=7.2), and 0.1% urea (Merck, Germany). After five days, the bacteria were harvested, dried at room temperature (25°C), and autoclaved for 15 minutes at 121°C. The PVKU-derived biomass was incinerated at 600°C for two hours in a furnace (Nabertherm, Germany) to eliminate any biologically active material from the HA production (21). Then, the synthesised biomaterial was characterised. The dried bacterial biomass harvested from the PVKU medium was named PVKUS and the dried bacterial biomass harvested from the NA medium was named NAS. We used 1 mg/ml of PVKUS and NAS for the cell line treatments.

Characterisation of bacterial synthesised hydroxyapatite

Synthesised HA from *B. coagulans* grown on PVKU

medium was identified by X-ray diffraction (XRD, D8 Advance, Bruker, Germany) at 35 kV and 30 mA in reflection mode with Cu Kα (λ=1.540598 Å radiation) with a scanning speed of 0.04° s^{-1}, scanning electron microscopy (SEM), energy-dispersive X-ray (EDX) analysis at 20 kV (Philips XI30, The Netherlands), and Fourier transform infrared spectroscopy (FTIR; FT/IR-6300, JASCO Corp., Japan) in the chemical bond absorption range of 350-4000 cm^{-1} (21, 22).

3-(4,5-dimethylthiazol-2-yl)-2,5-diphenyltetrazolium bromide assay

SHED and the MG-63 cell line (donated by Professor Torabi Nejad Research Centre, Department of Dentistry, Isfahan University of Medical Sciences, Isfahan, Iran) were separately treated with 1 mg/ml PVKUS and 1 mg/ml NAS in Dulbecco's Modified Eagle Medium High Glucose [DMEM-H10% foetal bovine serum (FBS), 1% penicillin/streptomycin, Bio Idea] and incubated in a humidified atmosphere of 95% air and 5% CO_2 at 37ºC. The growth rate and viability of the cells were assessed by the 3-(4,5-dimethylthiazol-2-yl)-2,5-diphenyltetrazolium bromide (MTT) method after three, five, and seven days. The cell lines were subjected to viability analysis and compared to an untreated control group. The experimental procedure involved removing the medium from each well, washing the wells with PBS, and subsequently adding 400 µL of medium and 40 µL of MTT solution (5 mg/mL) to each well. After four hours of incubation at 37°C, the supernatant was removed, and 400 µL of dimethyl sulphoxide (DMSO, Sigma, USA) was added to each well. Following a 20-minute incubation in a dark room, the absorbance was measured at 590 nm using a multi-mode reader (Synergy HTX, USA) (23). The cell viability assay was performed in three replications. Then, the population doubling number (PDN) was determined by utilising the following formula:

$$PDN=\log (N/N_0)\times 3.31$$

In this equation, N represents the final population cell number after three, five, and seven days, and N0 represents the initial population number (24).

Osteoblastic differentiation of human exfoliated deciduous teeth

Characterisation of osteodifferentiation was performed by observed morphological changes, measurement of alkaline phosphatase (ALP) activity, and staining of calcium deposits with alizarin red. The osteoblastic differentiation study for SHED was conducted by treating SHED with an autoclaved sample from the PVKU medium (PVKUS). We added 2×10^4 SHED cells to each well of a six-well plate. PVKUS+DMEM-H medium were added to some of the wells. The negative control wells had only DMEM-H, whereas the positive control wells contained osteogenic medium (STEMCELL Technologies, Canada). The plate was maintained in a humidified atmosphere of 95% air and 5% CO_2 at 37ºC, and we changed the media every three days. After 7, 14, and 21 days we assessed for osteogenic differentiation by conducting the osteoblastic differentiation tests in triplicate (25, 26).

Morphological observation

The changes in SHED cell morphology were checked following osteogenic differentiation across three-time points (7, 14, and 21 days) under an inverted microscope (Motic AE31, China). Images of the cell changes were captured.

Alizarin red staining

After 21 days of osteogenesis induction, the cells were subjected to alizarin red staining to investigate the presence of calcium deposits for bone nodule formation. First, the cells were fixed in 400 µL of 10% formaldehyde for 30 minutes and then washed twice with PBS. Next, 400 µL of a 2% alizarin red stain (pH=4.2) solution was added to each well and the plate was allowed to incubate at room temperature for 15 minutes. After incubation, the solution was aspirated, and the cells were washed with distilled water. The stained cells were then observed under light microscopy, and images were captured. In order to quantitatively determine the optical density, 400 µL of 10% acetic acid was placed in each well and left to incubate for 30 minutes. Subsequently, the cell layer was gently scraped and combined with acetic acid in a microtube, and thoroughly mixed by vortexing. The sample was then heated at 85°C for 10 minutes, cooled on ice, and finally centrifuged at 20 000 g for 15 minutes. The resulting supernatant was carefully transferred to a 96-well plate, and the optical density (OD) value was measured at a single wavelength of 405 nm (27, 28).

Alkaline phosphatase activity

For osteogenic differentiation, we used the ALP assay. At 7, 14, and 21 days of culture, we removed the medium and rinsed the cells with PBS in order to eliminate any residual culture medium. The cells were trypsinised, placed in a falcon tube, and centrifuged at 300 g for 10 minutes. The supernatant was removed and cells were washed with PBS. Then, 200 µl of 0.8% (v/v) Triton x100 was added to a falcon tube for cell lysis to rupture the cell membranes and release the ALP molecules. The tubes were subjected to two rounds of centrifugation at 1600 g and 4°C for 10 minutes each in order to evaluate ALP activity. Approximately 10 µl of cell extract was added to each well of the 96-

well plates. Subsequently, each 96-well plate received the following additions: 40 µl of magnesium sulphate (w/v), 10 µl of p-nitrophenyl phosphate (w/v), and 40 µl of bicarbonate-carbonate buffer ($NaNO_3$-Na_2CO_3) (w/v) with a pH of 10.0 (PARSAZMOON, Iran). Next, the cells were placed in a controlled environment at a temperature of 37°C and allowed to incubate for 30 minutes. Following the incubation period, 100 µl of NaOH was mixed with each sample to halt the enzymatic process. A spectrophotometer was employed to measure the OD at a wavelength of 405 nm. The ALP enzyme activity was quantified using a unit (U), where one unit represents the release of 1 µmol p-nitrophenol per minute at a temperature of 37°C (29).

Statistical analysis

In this study, we used descriptive statistics and presented the results in graph form. Statistical analysis was performed using a Prism statistical software package (GraphPad Software, Inc., La Jolla, CA, USA). Two-way ANOVA and Tukey multiple comparison tests were employed for mean comparison. A significance level of $P<0.05$ was considered statistically significant.

Results

Synthesis and characterisation of the bacterial hydroxyapatite

B. coagulans (ATCC 7050 Iranian Biological Resource Centre) was chosen due to its beneficial properties and widespread use as a probiotic in the food and medical industries (30). After cultivation on PVKU and NA media, the bacterial mass was harvested and dried. The consumption of calcium and insoluble phosphate from PVKU medium was observed by the presence of a clear zone that formed around the cultivation line on the cultural medium, a finding consistent with previous results (21). Based on this data, bacilli can synthesise biomaterials by biomineralising calcium and insoluble phosphate internally (31), which leads to purification of the biomineralised biomaterial for further investigations.

X-ray diffraction analysis

XRD patterns indicate that the synthesised HA peaks (Fig.1A) align with the standard XRD graph reference of the International Centre for Diffraction Data (ICDD) for HA (09-0432) as depicted in Figure 1B (22). Crystallinity of the synthesised HA was confirmed by the preference for orientation along the (211) and (212) planes. The Scherer equation was used to determine crystal size from the XRD peaks (22) and indicated the HA size to be 80-100 nm. The results corroborate the ability of probiotic *B. coagulans* to produce HA in a PVKU medium, as established in our previous study (21).

Scanning electron microscopy imaging and energy-dispersive X-ray analysis

SEM images (Fig.2A) revealed the braided morphological features of bacterial HA and the crystal size of the HA (range: 80-100 nm). The elemental composition and Ca/P ratios of HA were determined by EDX. The Ca/P ratio was 1.9, which was close to the stochiometric human bone HA ratio (Fig.2B).

Fourier transform infrared spectroscopy

The Fourier transform infrared spectroscopy (FTIR) spectrum of the synthesised HA (Fig.2C) showed the presence PO_4^{3-}, OH^-, and CO_3^{2-} chemical groups, all typical of conventional HA (32, 33). Strong IR absorption bands were exhibited by the PO_4^{3-} group at 400-700 cm^{-1} and 1000-1100 cm^{-1}. The adsorbed water band was broad, and spanned from 2000 to 3000 cm^{-1}, with a distinct peak at 3427 cm^{-1} and a weaker peak at 1800 cm^{-1}. CO_3^{2-} peaks that corresponded to the natural HA were observed between 1400 and 1500 cm^{-1} (34).

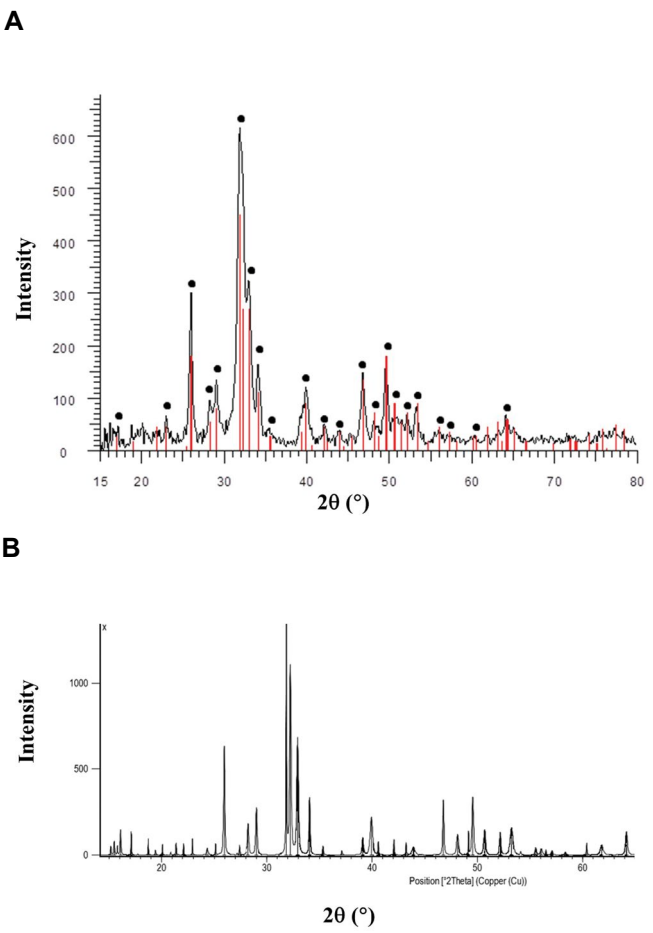

Fig.1: X-ray diffraction of synthesized HA. **A.** XRD pattern of *Bacillus coagulans (B. coagulans)* mediated HA. **B.** ICDD database for the standard peak of HA. XRD; X-ray diffraction, HA; hydroxyapatite, ICDD; International Centre for Diffraction Data, and ·; Hydroxyapatite.

Cell viability

The effects of NAS and PVKUS on the viability and the proliferation rate of the SHED and MG-63 lines were examined by MTT. The results are reported as the OD of the viable cells compared to the untreated SHED control. Figure 3A and B show cellular viability and PDN for SHED. Figure 3C and D depict the graphs for cellular viability and PDN of the MG-63 cells. These graphs represent the data obtained after culturing both cell types for three, five, and seven days. ANOVA findings confirmed that NAS and PVKUS did not show any toxicity and had highly significant ($P<0.001$) growth induction (14 and 33%, respectively) on SHED. PVKUS was significantly more effective than NAS in increasing MG-63 cell viability. The cell PDN calculated for NAS and PVKUS showed that the PDN (Fig.3B, D) was significantly higher for cells treated with PVKUS compared to the control and cells treated with NA ($P<0.001$). Therefore, we chose PVKUS for osteoblastic differentiation of stem cells because of its significantly more proliferative effect on the SHED and MG-63 cell lines.

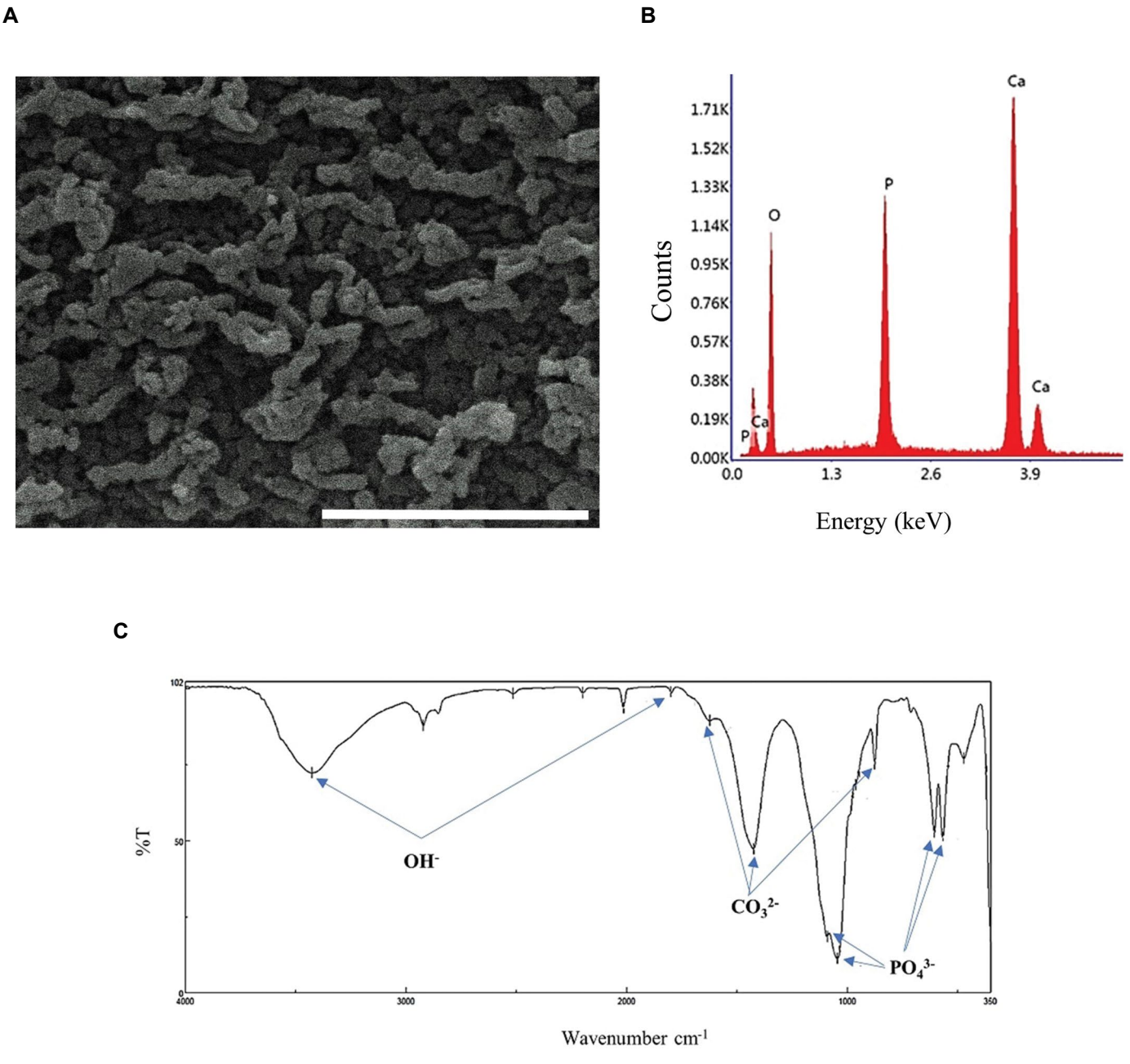

Fig.2: Characterisation of bacterial HA. **A.** SEM micrographs (scale: 300 nm). **B.** EDX graph and **C.** FTIR spectra graph of obtained probiotic bacterial nano HA from *Bacillus coagulans (B. coagulans).* SEM; Scanning electron microscopy, EDX; Energy-dispersive X-ray, FTIR; Fourier transform infrared spectroscopy, and HA; hydroxyapatite.

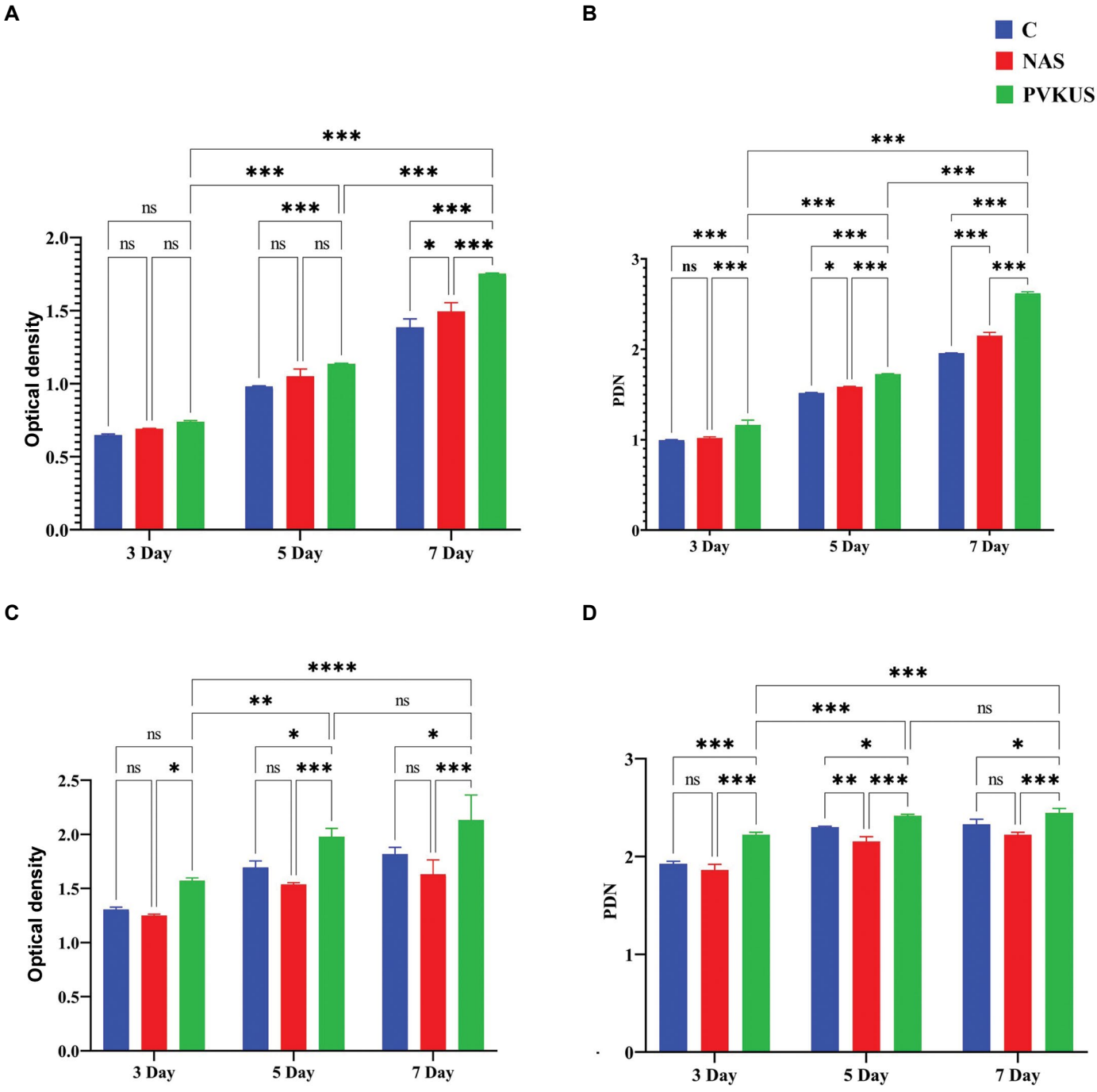

Fig.3: Cell viability. **A, B.** The effect of NAS and PVKUS [samples grown on NA and PVKU media, respectively] on SHED and **C, D.** MG-63 cell line viability. 3-(4,5-dimethylthiazol-2-yl)-2,5-diphenyltetrazolium bromide (MTT) reduction assays were used to evaluate cells treated with the same dose at different time points. The results revealed differences in OD between the treated and control cells. Untreated cells are considered as the control. Data are expressed as the mean ± SD. Statistical analysis is obtained from the results of two-way ANOVA. *; P<0.1, **; P<0.01, ***; P<0.001, ****; P<0.0001, ns; Not significant, NA; Nutrient agar, PVKU; Pikovskaya plus urea, SHED; Human exfoliated deciduous teeth, and OD; Optical density.

Osteoblastic differentiation of human exfoliated deciduous teeth

Morphological observation

Cellular shape is a significant indicator for characterising and evaluating cell quality (35). For osteogenic differentiation, we treated the SHED cell line with PVKUS and assessed the morphological alterations. The SHED cell lines cultured in osteogenic medium and basic DMEM-H medium were considered to be the positive and negative controls, respectively. We observed a spindle-shaped morphology and high capacity to attach to plastic surface in the DMEM-H medium. After five days, some of the cells treated with PVKUS began to change their morphology from spindle-shaped to a stellate shape and appeared more polygonal, which would be an osteocyte-associated feature (36). There was a homogeneous population of polygonal cells in the treated cells after four and 21 days of incubation

(Fig.4G-I); also, we observed a similar morphological variation in the SHED cell line in osteogenic medium (Fig.4D-F). However, there was no observed changed in morphology detected in the SHED cell line grown in DMEM-H medium (Fig.4A-C).

Alizarin red staining

Mineral nodule formation is frequently employed as a means to evaluate the osteogenic differentiation of SHED. Alizarin red staining serves as an indicator of nodules that resemble mineralised structures. In this study, we used alizarin red to stain the intracellular calcium. This staining method is widely recognized for its utility in evaluating bone differentiation and as a marker for mineralisation (27). The visualization of a coloured complex within the cells indicated successful osteoblastic differentiation of SHED and the presence of a newly formed mineralised matrix (Fig.5). Alizarin red staining indicated that SHED grown in osteogenic medium and PVKUS significantly ($P<0.001$) created a calcified matrix after 21 days of culture. The undifferentiated control SHED grown in DMEM-H medium showed no alizarin red staining.

Alkaline phosphatase activity

The results of two-way ANOVA show that the ALP activity of the SHED group treated with PVKUS (0.181 ± 0.002 U/mg) was significantly higher than the SHED group treated with primary DMEM medium (0.021 ± 0.006 U/mg) and was equal to the SHED group treated with osteogenic medium (0.181 ± 0.001 U/mg) after 21 days ($P<0.001$). No significant increase in ALP levels was observed in cells treated with basic DMEM-H medium during 21 days (Fig.6). The results were similar to other researchers' findings that showed increased ALP levels during SHED differentiation (29).

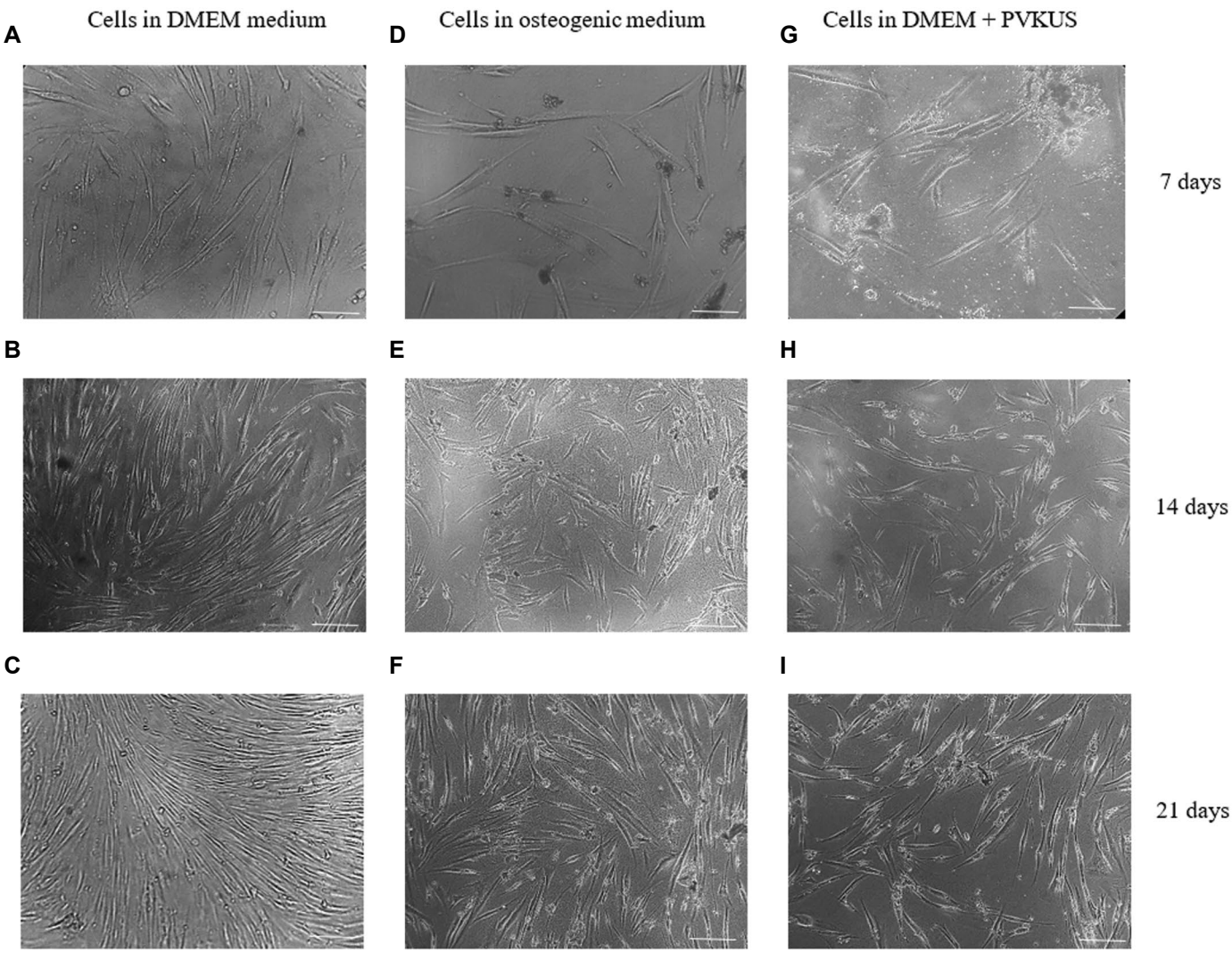

Fig.4: Cell morphological alteration during differentiation. **A-C.** SHED cultured in DMEM-H medium is the negative control (scale bar: 100 µm), **D-F.** SHED cultured in osteogenic medium is the positive control, and **G-H.** Morphological changes of SHED during osteogenic differentiation from a spindle-shape to stellate-shaped polygon as observed by phase-contrast microscopy after 7, 14, and 21 days. SHED; Human exfoliated deciduous teeth, DMEM; Dulbecco's Modified Eagle Medium, and PVKU; Pikovskaya plus urea.

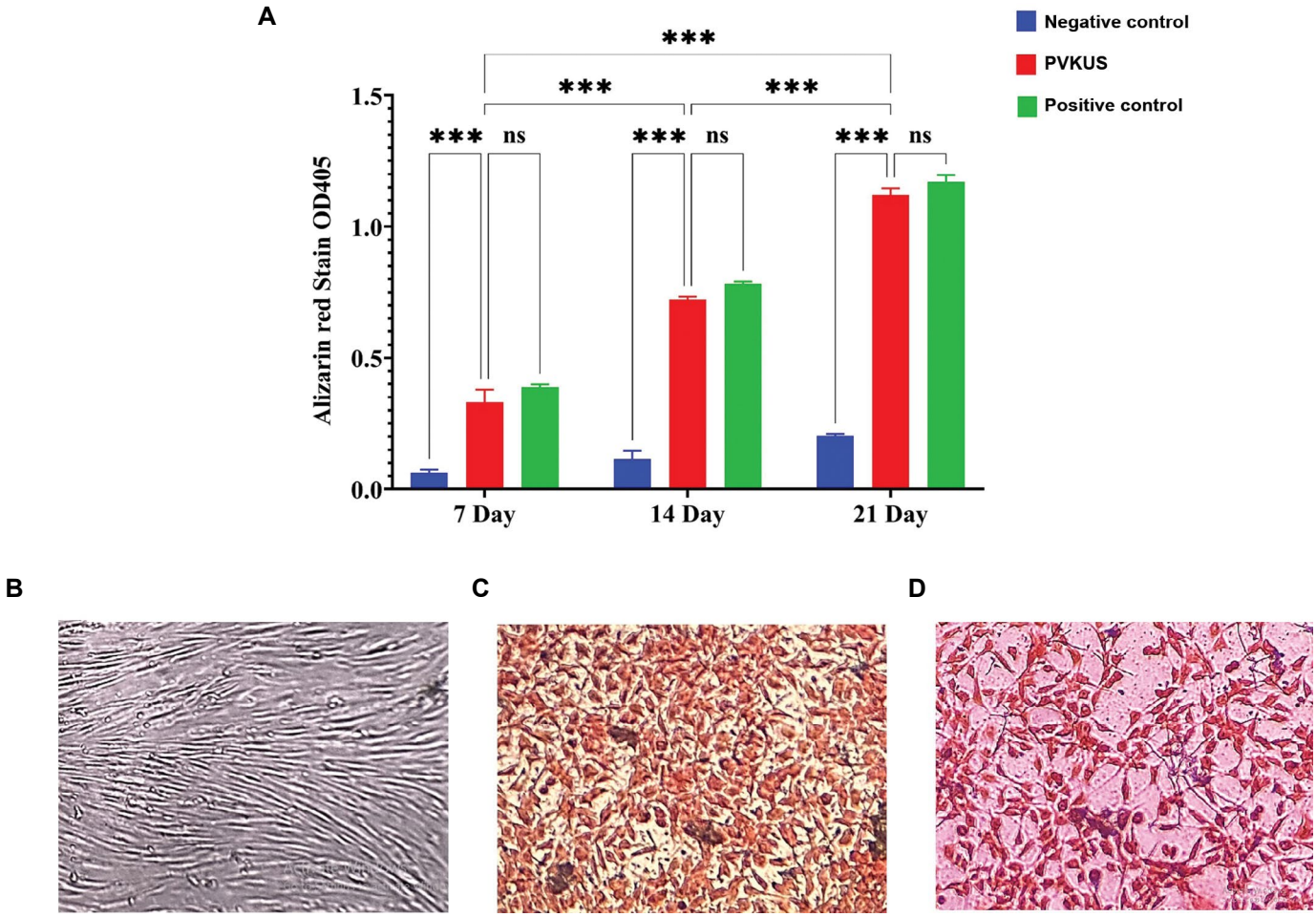

Fig.5: Alizarin red-stained mineralized nodules formed by differentiated cells. **A.** Quantitative measurement, **B.** Normal culture medium containing DMEM supplemented with 10% FBS is the negative control, **C.** The formation of a coloured complex within the cells shows osteoblastic differentiation of SHED with PVKUS [debris of the cultured *Bacillus coagulans* (*B. coagulans*) on PVKU medium], and **D.** Cells cultured with an osteogenic differentiation medium are the positive control (scale bar: 30 µm). Statistical analysis is obtained from the results of two-way ANOVA. The results are expressed as mean ± SD. ***; P<0.001, ns; Not significant, DMEM; Dulbecco's Modified Eagle Medium, FBS; Fetal bovine serum, SHED; Human exfoliated deciduous teeth, and PVKU; Pikovskaya plus urea.

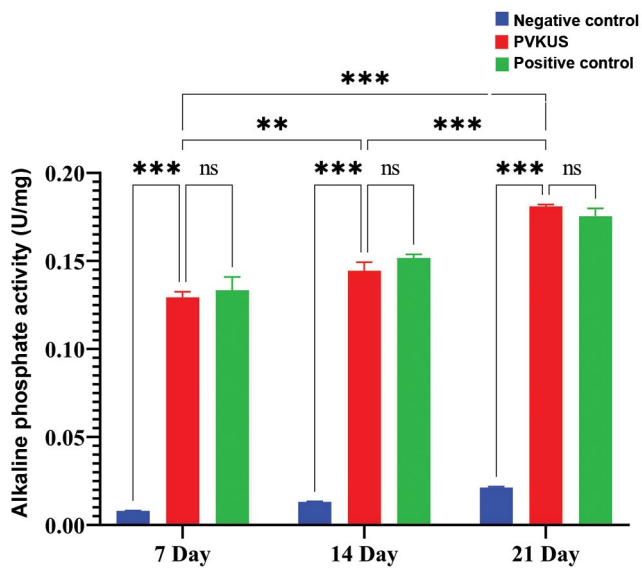

Fig.6: ALP activity of the SHED with PVKUS [debris of the cultured *Bacillus coagulans* (*B. coagulans*) on PVKU medium]. SHED cultured with DMEM-H without treatment is the negative control and SHED grown in osteogenic medium is the positive control. Data are expressed as mean ± SD. Statistical analysis obtained from results of two-way ANOVA. **; P<0.01, ***; P<0.001, ns; Not significant, ALP; Alkaline phosphatase, SHED; Human exfoliated deciduous teeth, PVKU; Pikovskaya plus urea, and DMEM-H; Dulbecco's Modified Eagle Medium High Glucose.

Discussion

In this investigation, the probiotic *B. coagulans* was utilised to biosynthesize nano-HA. The XRD pattern results exhibited sharp peaks, which confirmed crystallisation of the bio-organic phase on the surface of HA that were stabilised by bacteria that acted as chelating agents (31). SEM images revealed a braided or woven particle morphology with clumped distributions in a uniform nanoscale dimension that indicated consistent crystal development within the bacteria. Woven HA is typically found in bone structure, as well as in fractures and pathological situations, and it represents the first bone type to form during initial bone formation (32). Previous research has suggested the necessity of nanoscale HA for the human bone tissue surface and textural suitability for defective bone replacement (37). The presence of typical chemical groups of standard HA in the synthesised nano-HA, as confirmed by FTIR spectra, corroborate this characterisation (32-34). *B. coagulans*, a potential probiotic, has the capability to consume insoluble phosphate and calcium from the culture medium to synthesise HA crystals. This was evidenced by the identification of the purified powder from grown bacteria on PVKU medium. The formation of calcite and HA nanocrystals were reported previously in pathogenic bacteria and a limited number of non-pathogenic bacteria (21, 31).

Studies conducted on MG-63 cell cultures provided evidence that support the effectiveness of probiotics and HA. The results of these studies have shown that when probiotics were administered to MG-63 cells, they underwent increased proliferation and differentiation, which suggested their commitment to osteoblasts. MG-63 cells are commonly used as a model to study the viability, adhesion, and proliferation of bone cells. Moreover, the literature confirms that the MG-63 cell line maintains a stable phenotype and closely resembles human MSCs (20). This resemblance has significantly contributed to the widespread use of MG-63 cells in evaluating the compatibility of biomaterials intended for orthopaedic purposes and exploring bone metabolism that concerns osteoblast-like cells.

Recent studies have shown that debris from *Bacillus* sp. is not toxic to stem cells, while exhibiting inhibitory effects on cancerous cells (38). The surfactin production of *Bacillus* species, which was reported to stimulate cell proliferation and differentiation in some studies, was also noteworthy. It enhanced the production of hypoxia-inducible factor-1α and vascular endothelial growth factor, increased the movement of keratinocytes through the mitogen-activated protein kinase, Wnt/β-catenin pathway and nuclear factor-κB signalling pathways, and controlled the release of inflammatory cytokines and the change in macrophage phenotype (23). Given that the PVKUS and MG-63 stimulated greater proliferation in SHED in this investigation, it became clear that the HA synthesised from bacteria impacted cell multiplication in a way not reported in previous studies. Nano-HA acts as a catalyst for bone formation by promoting the differentiation and activity of osteoblasts through the provision of sufficient calcium and phosphate in the vicinity of SHED, thereby facilitating bone regeneration. Nano-HA, characterised by its small crystal size, creates higher levels of stress at the interface between cells and crystals compared to conventional flat-surfaced HA. The increased cell extension on the surface of nano-HA facilitates the exchange of calcium ions, which promotes the differentiation of MSC into osteoblasts. Furthermore, nano-HA can facilitate the attachment of specific cells that rely on surface adhesion by adsorbing extracellular matrix proteins such as fibronectin and growth factors like osteonectin (14, 39).

Morphological change serves as a marker of cell differentiation, as the cellular shape is a key factor in characterising and assessing cell quality (35). These morphological changes were consistent with previous research (40). While other studies investigating the osteogenic differentiation potential of stem cells have primarily employed cell-damaging techniques (such as staining, gene expression), assessing osteogenic potentiality using cellular morphology is a simple, direct, and non-invasive procedure. Several studies have revealed a relationship between osteogenic differentiation potentiality and cellular shape. Previous research has indicated that the stellate shape of stem cells is positively associated with the expression of osteogenic differentiation marker genes and the shape of osteocytes. It has been observed that cell geometry shows a significant correlation with the differentiation into osteogenic lineages (26, 35). Intracellular calcium deposits stained by alizarin red and the increase in ALP levels in cells during treatment with synthesised HA confirmed cell differentiation. Calcium deposits particularly found in bone tissues and ALP activity are significant indicators of early bone cell differentiation. These findings align with previous studies that used alizarin red staining to ascertain osteoblastic maturation and mineralisation (29). In recent studies, there has been a focus on exploring strategies that involve probiotic bacteria and their components to influence the proliferation and differentiation of MSCs. Additionally, it has been reported that HA can facilitate the differentiation of stem cells into osteogenic cells, which makes it a valuable component in tissue engineering. The present study successfully generated HA from probiotics, providing dual advantages in terms of its effects on stem cells and its potential application in tissue engineering (11, 12).

We propose a differentiation mechanism by probiotic and synthesised HA. Osteogenic differentiation is induced by adding probiotic debris as specific chemical inducers or growth factors to the culture medium. The chemical inducers initiate a cascade of signalling pathways such as the Wnt/β-catenin pathway within the dental pulp stem cells. Activation of this pathway promotes the expression of genes related to osteogenesis. The activated signalling pathways stimulate the expression of genes associated

with osteogenic differentiation. These genes include transcription factors such as RUNX2, osterix, and bone morphogenetic proteins. The differentiated dental pulp stem cells, now known as osteocytes, begin to deposit synthesised bacterial HA. As the osteocytes continue to deposit the mineralised matrix, it gradually forms a network of bone tissue. Over time, the newly formed bone tissue undergoes maturation and remodelling, which involves the activity of osteoclasts and osteoblasts to maintain bone homeostasis. Some researchers have investigated differentiation through expression (27, 29) and others through assessment of enzymatic and phenotypic properties (25, 26). We also used the latter method in this work.

Conclusion

The results of this study demonstrated that neither probiotic debris nor bacterial HA showed any toxic effect on SHED; rather, they enhanced the proliferation rate of the stem cells. PVKUS induced osteogenic differentiation of the SHED, which was confirmed by MTT, ALP assay, alizarin red staining, and morphological observation. HA production by probiotic bacteria was confirmed by sintering the bacterial mass at 600°C to remove the organic matter, followed by analysis of the obtained powder by XRD, FTIR, and SEM. Probiotics are frequently used in cosmetics, sanitation, the food industry, nutritional supplements, and medicine, with proven benefits. The current research reveals a dual advantage of probiotics that produce HA nanoparticles. It has been demonstrated that *B. coagulans* could prevent and treat peri-implant diseases and oral-dental infections. Meanwhile, HA particles in sanitation, medicine, and food industries could be applied to repair bones and teeth. Thus, the direct usage of probiotics that produce HA is recommended for achieving both goals.

Acknowledgements

The authors wish to thank the University of Isfahan for financial support of this work. The authors declare that they have no conflict of interests.

Authors' Contributions

S.N.; Conceptualization, Methodology, Validation, Formal analysis, Investigation, and Writing - original draft. R.R.; Supervision, Resources, Writing - review and editing, Project administration, and Funding acquisition. G.E.; Conceptualization, Methodology, Supervision, and Resources. O.G., R.S.; Writing – review, editing, and validation. All authors read and approved the final submitted manuscript.

References

1. Zhao R, Chen S, Zhao W, Yang L, Yuan B, Ioan VS, et al. A bioceramic scaffold composed of strontium-doped three-dimensional hydroxyapatite whiskers for enhanced bone regeneration in osteoporotic defects. Theranostics. 2020; 10(4): 1572-1589.
2. Pillai S, Upadhyay A, Khayambashi P, Farooq I, Sabri H, Tarar M, et al. Dental 3D-printing: transferring art from the laboratories to the clinics. Polymers (Basel). 2021; 13(1): 157-182.
3. Fang J, Li P, Lu X, Fang L, Lü X, Ren F. A strong, tough, and osteoconductive hydroxyapatite mineralized polyacrylamide/dextran hydrogel for bone tissue regeneration. Acta Biomater. 2019; 88: 503-513.
4. Shi H, Zhou Z, Li W, Fan Y, Li Z, Wei J. Hydroxyapatite based materials for bone tissue engineering: a brief and comprehensive introduction. Crystals. 2021; 11(2): 149-167.
5. Sudradjat H, Meyer F, Loza K, Epple M, Enax J. In vivo effects of a hydroxyapatite-based oral care gel on the calcium and phosphorus levels of dental plaque. Eur J Dent. 2020; 14(02): 206-211.
6. Babayevska N, Woźniak-Budych M, Litowczenko J, Peplińska B, Jarek M, Florczak P, et al. Novel nanosystems to enhance biological activity of hydroxyapatite against dental caries. Mater Sci Eng C Mater Biol Appl. 2021; 124: 112062.
7. Kantharia N, Naik S, Apte S, Kheur M, Kheur S, Kale B. Nano-hydroxyapatite and its contemporary applications. J Dent Res Sci Dev. 2014; 1(1): 15.
8. Nouri S, Roghanian R, Emtiazi G. Review on biological synthesis of nano-hydroxyapatite and its application in nano-medicine. Iran J Med Microbiol. 2021; 15(4): 369-383.
9. Aleixandre-Tudó JL, Castelló-Cogollos L, Aleixandre JL, Aleixandre-Benavent R. Tendencies and challenges in worldwide scientific
10. research on probiotics. Probiotics antimicrob proteins. 2020; 12(3): 785-797. Behera J, Ison J, Voor MJ, Tyagi N. Probiotics stimulate bone formation in obese mice via histone methylations. Theranostics. 2021; 11(17): 8605-8623.
11. Mendi A, Aktaş B, Aslım, B. Mesenchymal stem cell-probiotic communication: beneficial bacteria in preconditioning. In: Haider KH, ed. Handbook of stem cell therapy. Singapore: Springer Nature Singapore; 2022; 1-20.
12. Yan Q, Cai L, Guo W. New advances in improving bone health based on specific gut microbiota. Front Cell Infect Microbiol. 2022; 12: 821429.
13. Zaiss MM, Jones RM, Schett G, Pacifici R. The gut-bone axis: how bacterial metabolites bridge the distance. J Clin Invest. 2019; 129(8): 3018-3028.
14. Karbalaie KH, Tanhaei S, Rabiei F, Kiani-Esfahani A, Masoudi NS, Nasr-Esfahani MH, et al. Stem cells from human exfoliated deciduous tooth exhibit stromal-derived inducing activity and lead to generation of neural crest cells from human embryonic stem cells. Cell J. 2021; 23(1): 140-142.
15. Bhandi S, Alkahtani A, Mashyakhy M, Abumelha AS, Albar NHM, Renugalakshmi A, et al. Effect of ascorbic acid on differentiation, secretome and stemness of stem cells from human exfoliated deciduous tooth (SHEDs). J Pers Med. 2021; 11(7): 589.
16. Baghban EM, Bagheri F, Zandi M, Nejati E, Zomorodian E. Study of mesenchymal stem cell proliferation and bone differentiation on composite scaffolds of PLLA and nano hydroxyapatite with different morphologies. Cell J. 2011; 12(4): 469-476.
17. Miura M, Gronthos S, Zhao M, Lu B, Fisher LW, Robey PG, et al. SHED: stem cells from human exfoliated deciduous teeth. Proc Natl Acad Sci USA. 2003; 100(10): 5807-5812.
18. Hayashi Y, Kato H, Nonaka K, Nakanishi H. Stem cells from human exfoliated deciduous teeth attenuate mechanical allodynia in mice through distinct from the siglec-9/MCP-1-mediated tissue-repairing mechanism. Sci rep. 2021; 11(1): 20053.
19. Blokhuis TJ, Arts JJ. Bioactive and osteoinductive bone graft substitutes: definitions, facts and myths. Injury. 2011; 42 Suppl 2: S26-S29.
20. Mullick P, Das G, Aiyagari R. Probiotic bacteria cell surface-associated protein mineralized hydroxyapatite incorporated in porous scaffold: in vitro evaluation for bone cell growth and differentiation. Mater Sci Eng C Mater Biol Appl. 2021; 126: 112101.
21. Nouri S, Roghanian R, Emtiazi G, Shafiei R. Biosynthesis of nano-calcite and nano-hydroxyapatite by the probiotic bacteria of bacillus subtilis and bacillus coagulans. Appl Food Biotechnol. 2022; 9(4): 275-286.
22. Murugesan V, Vaiyapuri M, Murugeasan A. Fabrication and characterization of strontium substituted chitosan modify hydroxyapatite for biomedical applications. Inorg Chem Commun. 2022; 142: 109653.
23. Yan L, Liu G, Zhao B, Pang B, Wu W, Ai C, et al. Novel biomedical functions of surfactin A from Bacillus subtilis in wound healing promotion and scar inhibition. J Agric Food Chem. 2020; 68(26): 6987-6997.
24. Cerci E, Erdost H. Phenotypic characterization and differentiation of mesenchymal stem cells originating from adipose tissue. Turk J Vet Anim Sci. 2019; 43(6): 834-845.

25. Tetè G, Capparè P, Gherlone E. New application of osteogenic differentiation from HiPS stem cells for evaluating the osteogenic potential of nanomaterials in dentistry. Int J Environ Res Public Health. 2020; 17(6): 1947.
26. KarbalaeiMahdi A, Moridi K, Ghollasi M. Evaluation of osteogenic differentiation of human mesenchymal stem cells (hMSCs) on random and aligned polycaprolactone-polyaniline-gelatin scaffolds. BioImpacts. 2023; 13(2): 123-132.
27. Su WT, Wu PS, Huang TY. Osteogenic differentiation of stem cells from human exfoliated deciduous teeth on poly (ε-caprolactone) nanofibers containing strontium phosphate. Mater Sci Eng C Mater Biol Appl. 2015; 46: 427-434.
28. Khorolsuren Z, Lang O, Pallinger E, Foldes A, Szabolcs GG, Varga G, et al. Functional and cell surface characteristics of periodontal ligament cells (PDLCs) on RGD-synthetic polypeptide conjugate coatings. J Periodontal Res. 2020; 55(5): 713-723.
29. Hagar MN, Yazid F, Luchman NA, Ariffin SHZ, Wahab RMA. Comparative evaluation of osteogenic differentiation potential of stem cells derived from dental pulp and exfoliated deciduous teeth cultured over granular hydroxyapatite based scaffold. BMC Oral Health. 2021; 21(1): 263.
30. Adibpour N, Hosseininezhad M, Pahlevanlo A, Hussain MA. A review on Bacillus coagulans as a Spore-Forming Probiotic. Appl Food Biotechnol. 2019; 6(2): 91-100.
31. Ghashghaei S, Emtiazi G. Production of hydroxyapatite nanoparticles using tricalcium-phosphate by alkanindiges illinoisensis. J Nanomater Mol Nanotechnol. 2013; 2(5).
32. Esmaeilkhanian A, Sharifianjazi F, Abouchenari A, Rouhani A, Parvin N, Irani M. Synthesis and characterization of natural nano-hydroxyapatite derived from turkey femur-bone waste. Appl Biochem Biotechnol. 2019; 189(3): 919-932.
33. Elbasuney S. Green synthesis of hydroxyapatite nanoparticles with controlled morphologies and surface properties toward biomedical applications. J Inorg Organomet Polym Mater. 2020; 30(12): 899-906.
34. Núñez D, Elgueta EY, Varaprasad K, Oyarzún P. Hydroxyapatite nanocrystals synthesized from calcium rich bio-wastes. Mater Lett. 2018; 230: 64-68.
35. Kelly DJ, Jacobs CR. The role of mechanical signals in regulating chondrogenesis and osteogenesis of mesenchymal stem cells. Birth Defects Res C Embryo Today. 2010; 90(1): 75-85.
36. Escobar LM, Bendahan Z, Bayona A, Castellanos JE, González MC. Effect of vitamins D and E on the proliferation, viability, and differentiation of human dental pulp stem cells: an in vitro study. Int J Dent. 2020; 2020: 8860840.
37. Armiento AR, Hatt LP, Sanchez Rosenberg G, Thompson K, Stoddart MJ. Functional biomaterials for bone regeneration: a lesson in complex biology. Adv Funct Mater. 2020; 30(44): 1909874.
38. Asadi S, Soleimani N. Anticancer effect of fractions from staphylococcus aureus and bacillus atrophaeus on the proliferation and death of human breast cancer cell line (MCF-7). Int J Enteric Pathog. 2020; 8(4): 116-121.
39. Liang W, Ding P, Li G, Lu E, Zhao Z. Hydroxyapatite nanoparticles facilitate osteoblast differentiation and bone formation within sagittal suture during expansion in rats. Drug Des Devel Ther. 2021; 15: 905-917.
40. Wang X, Li G, Liu Y, Yu W, Sun Q. Biocompatibility of biological material polylactic acid with stem cells from human exfoliated deciduous teeth. Biomed Rep. 2017; 6(5): 519-524.